ANALYSIS OF REAL VECTOR FIELDS ON THE SPHERE USING SLEPIAN FUNCTIONS

Alain Plattner[1], *Frederik J. Simons*[1], *Liying Wei*[2]

[1] Princeton University, Department of Geosciences
[2] Chinese University of Hong Kong, Department of Electronic Engineering

ABSTRACT

We pose and solve the analogue of Slepian's time-frequency concentration problem for vector fields on the surface of the unit sphere, to determine an orthogonal family of strictly bandlimited vector fields that are optimally concentrated within a closed region of the sphere or, alternatively, of strictly spacelimited functions that are optimally concentrated in the vector spherical harmonic domain. Such a basis of simultaneously spatially and spectrally concentrated functions should be a useful data analysis and representation tool in a variety of geophysical and planetary applications, as well as in medical imaging, computer science, cosmology, and numerical analysis.

Index Terms— Spherical vector fields, spatiospectral concentration, prolate spheroidal wave functions

1. INTRODUCTION

Functions cannot be simultaneously bandlimited and spacelimited to a region of interest. It is possible, however, to design functions that are bandlimited, but optimally concentrated with respect to their spatial energy inside the target region.

In a classic series of papers published in the 1960s, Slepian, Landau, and Pollak solved a fundamental problem in information theory, namely, that of optimally concentrating a given signal in both the time and frequency domains [1, 2, 3, 4]. The orthogonal family of data windows, or tapers, that arise in this context, and their discrete and multidimensional extensions, are used in the multitaper method of spectral analysis, which has enjoyed application in a wide range of physical, computational, and biomedical disciplines, and form the basis for function representation, approximation interpolation, and extension. Time-frequency and time-scale concentration in more general settings and a variety of geometries has subsequently been studied by several authors [5, 6].

A similar concept was brought to the sphere in terms of scalar spherical functions that are spatially concentrated while bandlimited [7, 8, 9, 10]. Since then, "Slepian functions" have been applied in fields as diverse as geodesy, geomagnetism, gravimetry, geodynamics, biomedical science, planetary science, and cosmology. Here we present the beginnings of a complete extension of Slepian's spatiospectral concentration problem to vector fields on the sphere, whereby we note that the first successful attempts at constructing spatially concentrated bandlimited tangential spherical vector fields have come from the field of magnetoencephalography [11, 12].

2. PRELIMINARIES

We denote the colatitude of spherical points $\hat{\mathbf{r}}$ by $0 \le \theta \le \pi$ and the longitude by $0 \le \phi < 2\pi$. The unit vector pointing outwards in the radial direction will be denoted by $\hat{\mathbf{r}}$, and the unit vectors in the tangential directions towards the south pole and towards the east will be denoted by $\hat{\boldsymbol{\theta}}$ and $\hat{\boldsymbol{\phi}}$, respectively. We use R to denote a region of the unit sphere Ω, of area $A = \int_R d\Omega$, within which we seek to concentrate a bandlimited vector field. The region may consist of a number of unconnected subregions, $R = R_1 \cup R_2 \cup \dots$, and it may have an irregularly shaped boundary. The region complementary to R will be denoted by $\Omega \setminus R$.

Restricting our attention to real-valued vector fields, we use real vector spherical harmonics, which are constructed from their scalar counterparts. Each scalar spherical harmonic Y_{lm} has a degree $0 \le l$ and, for each degree, an order $-l \le m \le l$. We choose our spherical harmonics to be unit-normalized in the sense [13]. From the scalar spherical harmonics we construct the vector spherical harmonics as

$$\begin{aligned} \mathbf{P}_{lm} &= \hat{\mathbf{r}} Y_{lm}, \\ \mathbf{B}_{lm} &= \frac{\boldsymbol{\nabla}_1 Y_{lm}}{\sqrt{l(l+1)}} = \frac{[\hat{\boldsymbol{\theta}}\partial_\theta + \hat{\boldsymbol{\phi}}(\sin\theta)^{-1}\partial_\phi] Y_{lm}}{\sqrt{l(l+1)}}, \\ \mathbf{C}_{lm} &= \frac{-\hat{\mathbf{r}} \times \boldsymbol{\nabla}_1 Y_{lm}}{\sqrt{l(l+1)}} = \frac{[\hat{\boldsymbol{\theta}}(\sin\theta)^{-1}\partial_\phi - \hat{\boldsymbol{\phi}}\partial_\theta] Y_{lm}}{\sqrt{l(l+1)}}, \end{aligned} \tag{1}$$

where again $0 \le l$ are the degrees and $-l \le m \le l$ the orders. The $\mathbf{P}_{lm}$ span the radial components and $\mathbf{B}_{lm}$ and $\mathbf{C}_{lm}$ the tangential components of the spherical vector field.

The expansion of a real bandlimited vector field $\mathbf{g}(\hat{\mathbf{r}})$ on the unit sphere Ω can be written in this basis as

$$\mathbf{g} = \sum_{lm}^{L} U_{lm}\mathbf{P}_{lm} + V_{lm}\mathbf{B}_{lm} + W_{lm}\mathbf{C}_{lm}, \tag{2}$$

where $\sum_{lm}^{L} := \sum_{l=0}^{L}\sum_{m=-l}^{l}$ whenever $\mathbf{P}_{lm}$ or U_{lm} are involved and $\sum_{lm}^{L} := \sum_{l=1}^{L}\sum_{m=-l}^{l}$ for $\mathbf{B}_{lm}$, $\mathbf{C}_{lm}$, V_{lm} or W_{lm}. The radial and tangential expansion coefficients U_{lm}, V_{lm} and W_{lm} are collected in the spectral vector g. The bandwidth is L.

3. SPATIAL CONCENTRATION

To maximize the spatial concentration within a region R of a bandlimited vector field $\mathbf{g}(\hat{\mathbf{r}})$, we maximize the ratio

$$\lambda = \frac{\|\mathbf{g}\|_R^2}{\|\mathbf{g}\|_\Omega^2} = \frac{\displaystyle\int_R (\mathbf{g}\cdot\mathbf{g})\, d\Omega}{\displaystyle\int_\Omega (\mathbf{g}\cdot\mathbf{g})\, d\Omega}. \tag{3}$$

The variational problem (3) is analogous to the one-dimensional problem [1] and the scalar spherical problem [7]. Here, as there, the ratio $0 < \lambda < 1$ is a measure of the spatial concentration. The maximization of (3) is equivalent to requiring that

$$\lambda = \frac{\mathsf{g}^{\mathsf{T}}\mathsf{K}\,\mathsf{g}}{\mathsf{g}^{\mathsf{T}}\mathsf{g}} = \text{maximum}, \tag{4}$$

978-1-4673-0183-1/12/$31.00

whereby the spectral-domain matrix

$$\mathsf{K} = \begin{pmatrix} \mathsf{P} & 0 & 0 \\ 0 & \mathsf{B} & \mathsf{D} \\ 0 & \mathsf{D}^\mathsf{T} & \mathsf{C} \end{pmatrix} \tag{5}$$

is composed of the matrix entries defined by

$$\mathsf{B}_{lm,l'm'} := \int_R \mathbf{B}_{lm} \cdot \mathbf{B}_{l'm'} \, d\Omega, \tag{6}$$

$$\mathsf{C}_{lm,l'm'} := \int_R \mathbf{C}_{lm} \cdot \mathbf{C}_{l'm'} \, d\Omega, \tag{7}$$

$$\mathsf{D}_{lm,l'm'} := \int_R \mathbf{B}_{lm} \cdot \mathbf{C}_{l'm'} \, d\Omega. \tag{8}$$

Problem (4) can be solved by satisfying

$$\mathsf{K}\mathsf{g} = \lambda \mathsf{g}. \tag{9}$$

Hence we can construct optimally concentrated functions using the coefficients obtained from (9) in the manner of (2). Since the optimization problem for the radial components is decoupled from the tangential optimization problem, it is possible to solve the two independently. The radial concentration problem is exactly equivalent to the scalar optimization problem on the sphere [7].

Solving the eigenvalue problem (9) does not only return the best-concentrated function associated with the largest eigenvalue, but an entire orthogonal basis equivalent to the bandlimited set of vector spherical harmonics, if we solve for all eigenvalues. The new basis of vector-valued Slepian functions can be ordered with respect to their energy concentration inside the region of interest. Usually, there is a number of well-concentrated ($\lambda \approx 1$) Slepian functions, followed by a transition to a number of Slepian functions that focus almost exclusively on the complement of the region ($\lambda \approx 0$). The number of well-concentrated Slepian functions can be approximated by the "Shannon number", $(L+1)^2 A/(4\pi)$ for the radial problem and $[2(L+1)^2 - 2]A/(4\pi)$ for the tangential problem [Plattner and Simons, *manuscript in preparation*].

4. VECTOR SLEPIAN FUNCTIONS

In the special case of spherical polar caps the entries of the kernel K in (5) have analytic expressions. Additionally, the matrix K assumes a block-diagonal shape. Each pair of vector spherical harmonic orders $\pm m$ leads to two blocks and the maximum block size is $2L \times 2L$. Hence the eigenvalue problem can be solved very efficiently. Figure 1 shows such an example, of a spherical polar-cap vector Slepian function for maximum degree $L = 18$, orders $m = \pm 1$ and a cap opening angle of $\Theta = 40°$.

For more general regions, as for example Earth's continents, the matrices B, C and D can no longer be assembled analytically due to their irregular shape. However, the decoupling of the radial and tangential problems still holds.

Figure 2 shows the ten best-concentrated tangential Slepian functions for Africa, with bandlimit $L = 18$. Figure 3 shows the concentration values λ for tangential Slepian functions constructed for a series of regions on Earth and for two different bandwidths L. With the tangential Slepian functions, each concentration value appears twice. Both Slepian functions associated with this concentration value share the same intensity pattern and their directions are pointwise perpendicular.

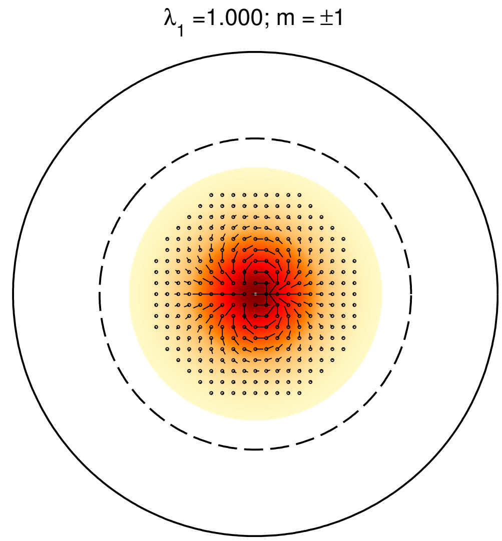

Fig. 1. Bandlimited tangential Slepian function $\mathbf{g}(\theta, \phi)$, of spherical harmonic orders $m = \pm 1$, optimally concentrated within a polar cap of radius $\Theta = 40°$. The dashed circle denotes the cap boundary. The bandwidth is $L = 18$. The color denotes the absolute value of the vector field, ranging from white for values below 1% of the maximum to red for the maximum value. The direction of the field is indicated by open circles and accordingly oriented strokes.

5. LOCALIZATION OF GLOBAL FIELDS

In order to demonstrate the spatial focusing capabilities of the bandlimited spatially optimized vector Slepian fields, we reconstruct a global tangential vector field, $\mathbf{u}$, by approximating it with fields $\mathbf{v}$ that use an increasing number, J, of vector Slepian functions

$$\mathbf{v} = \sum_{\alpha=1}^{J} u_\alpha \mathbf{g}_\alpha, \tag{10}$$

where the coefficients u_α are obtained by forming the inner product of $\mathbf{u}$ with the α best-concentrated vector Slepian functions $\mathbf{g}_\alpha$. The error over the domain, and the leakage to its complement, defined by

$$\text{error} = \sqrt{\frac{\|\mathbf{u}-\mathbf{v}\|_R^2}{\|\mathbf{u}\|_R^2}}, \quad \text{bias} = \sqrt{\frac{\|\mathbf{v}\|_{\Omega\setminus R}^2}{\|\mathbf{u}\|_{\Omega\setminus R}^2}}, \tag{11}$$

are used to assess the performance of the reconstruction. The error shows how far the reconstruction using only a limited number of Slepian fields strays from perfectly representing the original function; it decreases with increasing J. The bias captures the amount of bleeding into the complement to the domain R. It increases as the number of Slepian functions used gets larger. Our goal is to obtain a small reconstruction error within the region R while simultaneously keeping the outside leakage bias small.

Figure 4 shows the outcome of such an experiment conducted on a geophysical data set (the NGDC-720-V3 terrestrial crustal field model). The upper panel of Figure 5 shows the input tangential field expanded in all harmonics up to degree $L = 72$. The lower panel shows the reconstruction using the 924 best-concentrated tangential vector Slepian functions.

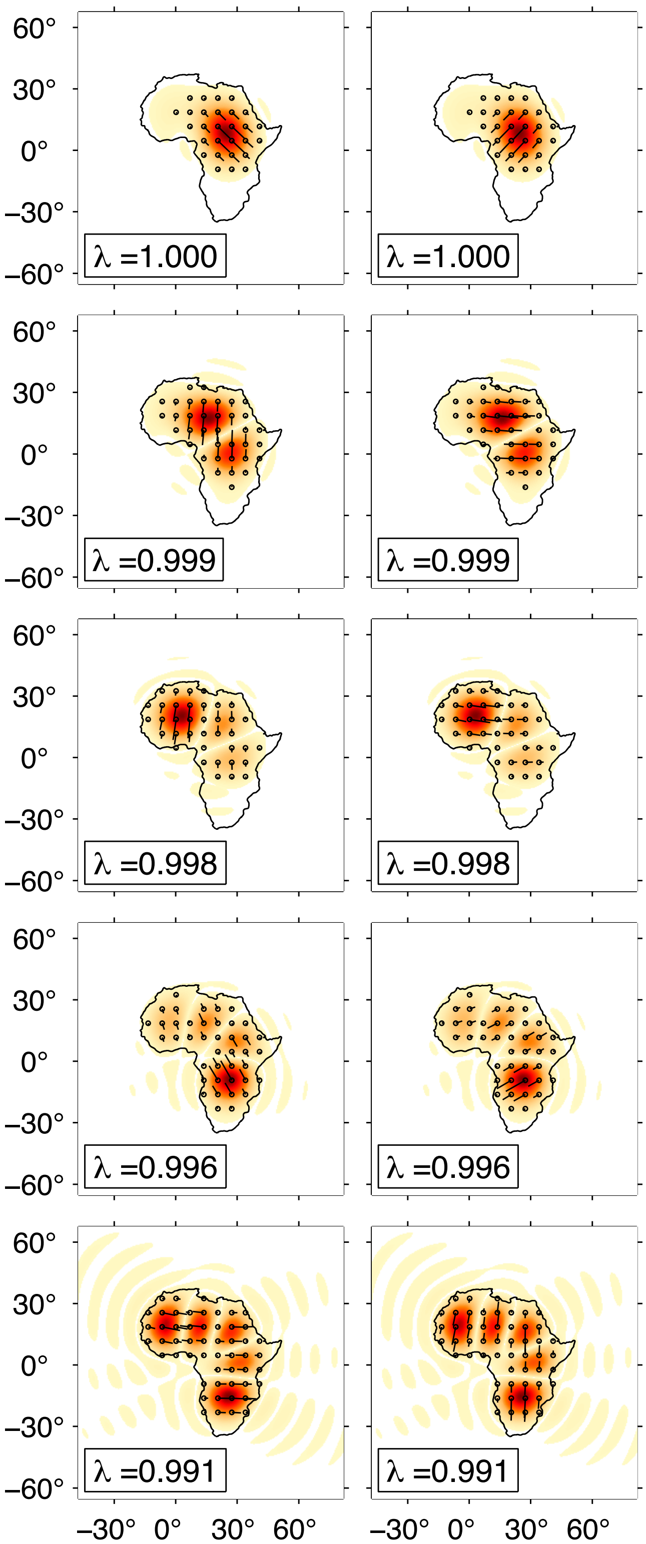

Fig. 2. Ten tangential Slepian functions, $g_1, g_2, \ldots, g_{10}$, bandlimited to $L = 18$, optimally concentrated within Africa. The concentration factors $\lambda_1, \lambda_2, \ldots, \lambda_{10}$ are indicated. The rounded Shannon number is $N = 42$. Order of concentration is left to right, top to bottom. Intensity and direction are rendered as in Figure 1.

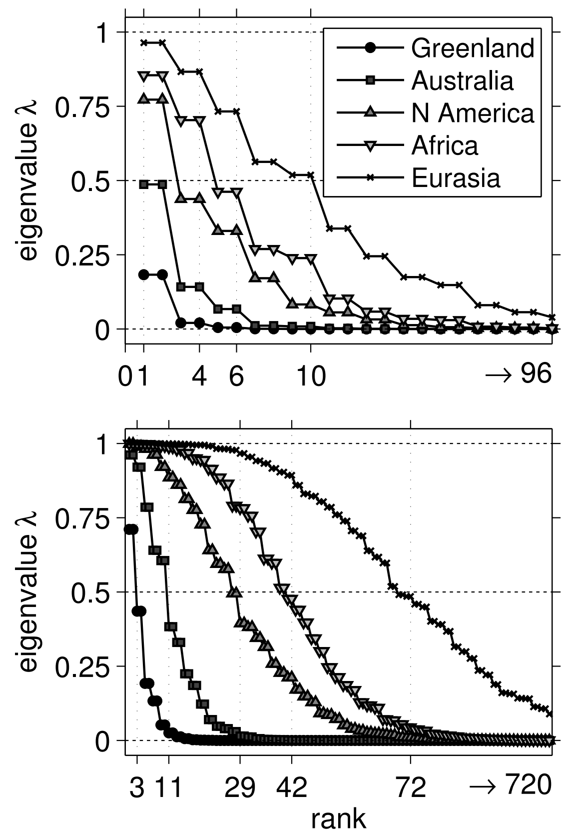

Fig. 3. Eigenvalue spectra for the tangential concentration problem to various continental regions. Two different bandwidths are considered, $L = 6$ (upper panel), and $L = 18$ (lower panel). The horizontal axis in each panel is truncated; the total number of eigenvalues $2(L+1)^2 - 2 = 96$, or 720, appears to the right of the arrow. Vertical grid lines and the five leftmost ordinate labels specify the rounded tangential Shannon numbers.

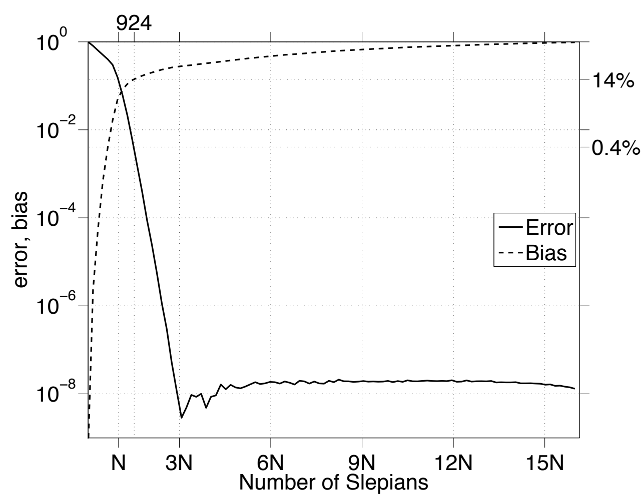

Fig. 4. Reconstruction error and bias over Africa, as defined in (11), versus the number of vector Slepian functions used to describe the global vector field shown in the upper panel of Figure 5, quoted as a multiple of the Shannon number, $N = 620$.

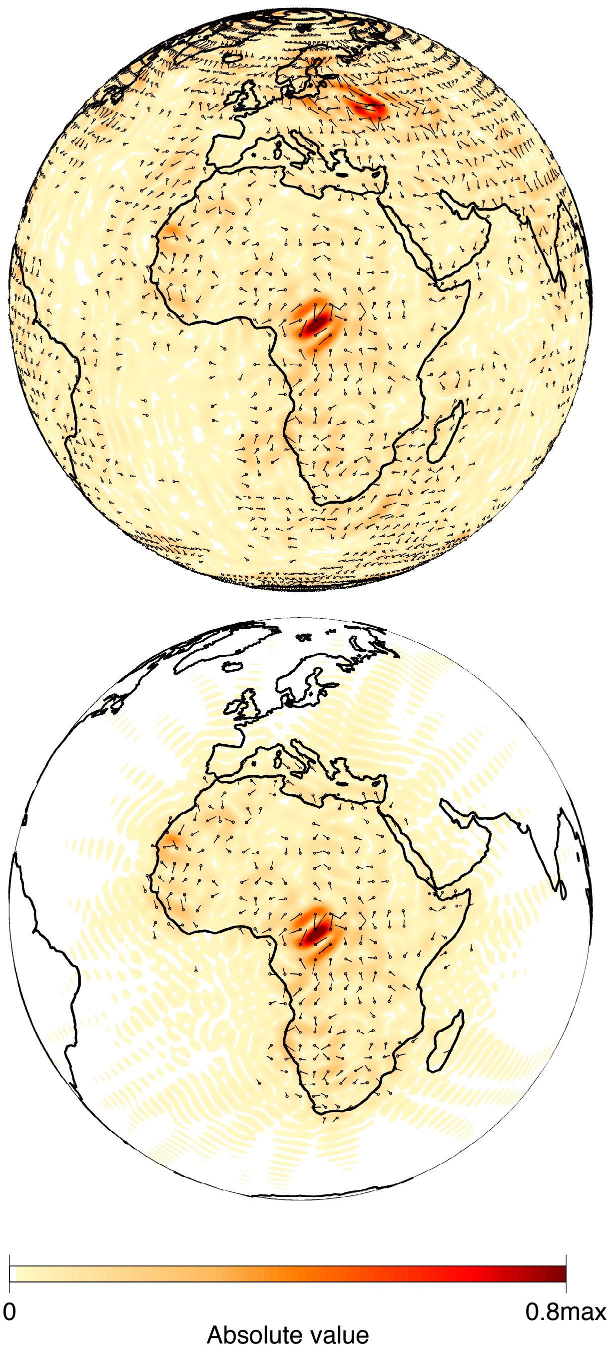

Fig. 5. A tangential geophysical vector field (top panel) and its reconstruction (bottom panel) using vectorial Slepian functions designed to maximize their spatial concentration in Africa. The bandlimit for both the original field and the Slepian basis, $L = 72$. There thus are 10656 vectorial basis functions in the original field, and the same number of Slepian functions from which to choose for the reconstruction. The bottom panel shows a reconstruction using the 924 best-concentrated Slepian functions for Africa. The error and bias over Africa, as defined in (11), are 0.4% and 14%, respectively. The Shannon number $N = 620$.

6. CONCLUSIONS

Vectorial Slepian functions on the sphere are an emerging tool for the analysis and representation of essentially space- and bandlimited vector-valued functions on the surface of the unit sphere. In this contribution we have sketched the key elements in their construction, shown various examples, and suggested their use in the constructive approximation of vectorial signals on the sphere, as may arise, for instance, in the fields of geophysics and planetary science. We expect that the impact of vectorial Slepian functions on multidimensional vectorial signal processing will be as profound as the classical prolate spheroidal wave functions have been, and continue to be, in the study of time series, and this in a wide variety of scientific and engineering fields.

7. REFERENCES

[1] D. Slepian and H. O. Pollak, "Prolate spheroidal wave functions, Fourier analysis and uncertainty – I," *Bell Syst. Tech. J.*, vol. 40, no. 1, pp. 43–63, 1960.

[2] H. J. Landau and H. O. Pollak, "Prolate spheroidal wave functions, Fourier analysis and uncertainty – II," *Bell Syst. Tech. J.*, vol. 40, no. 1, pp. 65–84, 1960.

[3] H. J. Landau and H. O. Pollak, "Prolate spheroidal wave functions, Fourier analysis and uncertainty – III dimension of space of essentially time- and band-limited signals," *Bell Syst. Tech. J.*, vol. 41, no. 4, pp. 1295–1336, 1962.

[4] D. Slepian, "Some comments on Fourier analysis, uncertainty and modeling," *SIAM Rev.*, vol. 25, no. 3, pp. 379–393, 1983.

[5] F. J. Simons, "Slepian functions and their use in signal estimation and spectral analysis," in *Handbook of Geomathematics*, W. Freeden, M. Z. Nashed, and T. Sonar, Eds., chapter 30, pp. 891–923, doi: 10.1007/978–3–642–01546–5_30. Springer, Heidelberg, Germany, 2010.

[6] F. J. Simons and D. V. Wang, "Spatiospectral concentration in the Cartesian plane," *Intern. J. Geomath.*, vol. 2, no. 1, pp. 1–36, doi: 10.1007/s13137–011–0016–z, 2011.

[7] F. J. Simons, F. A. Dahlen, and M. A. Wieczorek, "Spatiospectral concentration on a sphere," *SIAM Rev.*, vol. 48, no. 3, pp. 504–536, 2006.

[8] A. Albertella and F. Sacerdote, "Using Slepian functions for local geodetic computations," *Boll. Geod. Sc. Aff.*, vol. 60, no. 1, pp. 1–14, 2001.

[9] F. A. Grünbaum, L. Longhi, and M. Perlstadt, "Differential operators commuting with finite convolution integral operators: Some non-Abelian examples," *SIAM J. Appl. Math.*, vol. 42, no. 5, pp. 941–955, 1982.

[10] M. A. Wieczorek and F. J. Simons, "Localized spectral analysis on the sphere," *Geophys. J. Int.*, vol. 162, no. 3, pp. 655–675, 2005.

[11] H. Maniar and P. P. Mitra, "The concentration problem for vector fields," *Int. J. Bioelectromagn.*, vol. 7, no. 1, pp. 142–145, 2005.

[12] P. P. Mitra and H. Maniar, "Concentration maximization and local basis expansions (LBEX) for linear inverse problems," *IEEE Trans. Biomed Eng.*, vol. 53, no. 9, pp. 1775–1782, 2006.

[13] F. A. Dahlen and J. Tromp, *Theoretical Global Seismology*, Princeton University Press, Princeton, NJ, 1998.